Available online at www.sciencedirect.com
ScienceDirect
JOURNAL OF IRON AND STEEL RESEARCH, INTERNATIONAL. 2016, 23(9): 933-939

Mechanical Properties and Fracture Behavior of Cu-Co-Be Alloy after Plastic Deformation and Heat Treatment

Yan-jun ZHOU[1,2], Ke-xing SONG[2,3], Jian-dong XING[1], Zhou LI[4], Xiu-hua GUO[2,3]
(1. State Key Laboratory for Mechanical Behavior of Materials, School of Materials Science and Engineering, Xi'an Jiaotong University, Xi'an 710049, Shaanxi, China; 2. School of Materials Science and Engineering, Henan University of Science and Technology, Luoyang 471023, Henan, China; 3. Collaborative Innovation Center of Nonferrous Metals, Henan University of Science and Technology, Luoyang 471023, Henan, China; 4. School of Materials Science and Engineering, Central South University, Changsha 410083, Hunan, China)

Abstract: Mechanical properties and fracture behavior of Cu-0.84Co-0.23Be alloy after plastic deformation and heat treatment were comparatively investigated. Severe plastic deformation by hot extrusion and cold drawing was adopted to induce large plastic strain of Cu-0.84Co-0.23Be alloy. The tensile strength and elongation are up to 476.6 MPa and 18%, respectively. The fractured surface consists of deep dimples and micro-voids. Due to the formation of supersaturated solid solution on the Cu matrix by solution treatment at 950 ℃ for 1 h, the tensile strength decreased to 271.9 MPa, while the elongation increased to 42%. The fracture morphology is parabolic dimple. Furthermore, the tensile strength increased significantly to 580.2 MPa after aging at 480 ℃ for 4 h. During the aging process, a large number of precipitates formed and distributed on the Cu matrix. The fracture feature of aged specimens with low elongation (4.6%) exhibits an obvious brittle intergranular fracture. It is confirmed that the mechanical properties and fracture behavior are dominated by the microstructure characteristics of Cu-0.84Co-0.23Be alloy after plastic deformation and heat treatment. In addition, the fracture behavior at 450 ℃ of aged Cu-0.84Co-0.23Be alloy was also studied. The tensile strength and elongation are 383.6 MPa and 11.2%, respectively. The fractured morphologies are mainly candy-shaped with partial parabolic dimples and equiaxed dimples. The fracture mode is multi-mixed mechanism that brittle intergranular fracture plays a dominant role and ductile fracture is secondary.
Key words: Cu-Co-Be alloy; heat treatment; mechanical property; fracture behavior; plastic deformation

Beryllium copper (Cu-Be) alloys are the typical precipitation strengthened alloys. As a main strengthening element, the content range of Be element is 0.2—2.0 mass%[1,2]. The addition of cobalt element can prominently improve the mechanical strength, hardness, toughness, and resistance to high temperature of Cu-Be alloys. The Be element content range of high strength Cu-Be alloy is 1.6—2.0 mass%, while that of the high conductivity Cu-Be alloy is 0.2—0.6 mass%[3,4]. The mechanical properties of as-cast Cu-Be alloys can be improved through severe plastic deformation (forging, extrusion, drawing, etc.). After solution and subsequent aging treatment, the mechanical properties and electrical conductivity of Cu-Be alloys are improved significantly. Thus, severe plastic deformation methods can be widely used in the ocean engineering, defense industry, automobile industry, and petroleum industry, etc.[5-10].

Currently, the fracture behaviors and mechanical properties of stainless steel[11,12], aluminium alloy[13,14], magnesium alloy[15,16], and Cu-Zn alloys[17] etc. have been investigated. For the Cu-Be alloys, most investigations focused on the mechanical properties and fracture behaviors of high strength Cu-Be alloys (1.6—2.0 mass% Be)[4,5,7-9,18-29]. As referred by Sudhakar et al.[18] and Rosenthal[19], the fracture

Foundation Item: Item Sponsored by National Key Research and Development Program of China (2016YFB0301401); State Key Program of National Natural Science Foundation of China (U1502274); Innovation Scientists and Technicians Troop Construction Projects of Henan Province of China (C20150014); Program for Innovation Research Team (in Science and Technology) in University of Henan Province of China (14IRTSTHN007)
Biography: Yan-jun ZHOU, Doctor; **E-mail**: dazhou456@163.com; **Received Date**: November 24, 2015
Corresponding Author: Ke-xing SONG, Doctor, Professor; **E-mail**: kxsong@haust.edu.cn

behaviors under various loading modes of Cu-Be alloys were examined and the fracture mechanisms were analyzed; according to the results, the dominant failure mechanism was intergranular fracture under tensile mode. Jen et al.[20] investigated the effect of over-aging on fracture toughness of C17200 beryllium copper; meanwhile, the micro-fracture and macro-fracture behaviors of this alloy were comprehensively studied; by analyzing the fracture behavior, the internal relationship between pre-cracking fatigue propagation rate and fracture toughness was revealed. Millett[21] studied the effect of age hardening on the shock response of Cu-2.0 mass% Be alloy, and the results indicated that the shear strength of this alloy after solution treatment was nearly identical to that of pure copper, and the aging treatment significantly improved the strength under shock loading. However, the effects of preparation method and heat treatment on the mechanical properties and fracture behavior, as well as the fracture mechanism of Cu-Be alloys have been hardly investigated yet. Furthermore, there are few reports about the comparison of mechanical properties and fracture characteristic after plastic deformation and heat treatment for the Cu-Co-Be alloys (0.2 — 0.6 mass% Be). Therefore, the mechanical properties, fracture morphology, and microstructure characteristics of Cu-0.84Co-0.23Be alloy after plastic deformation, solid solution and aging treatment were investigated in this paper. Meanwhile, the fracture behavior at elevated temperature of aged Cu-0.84Co-0.23Be alloy was also researched.

1 Experimental Procedures

The electrolytic copper (99.99 mass%), cobalt flake (99.95 mass%), and Cu-3.3 mass% Be master alloy were used for preparing the Cu-0.8Co-0.2Be (nominal composition) ingot. The raw materials were melted in a KGPT200-2.5 medium frequency induction furnace at the temperatures of 1150—1250 ℃. The feeding sequence of raw materials was electrolytic copper, cobalt flake, and Cu-Be master alloy. The phosphor copper alloy was used for deoxidization. The molten metals were poured into a cast iron mould and an ingot with a diameter of 100 mm was obtained. The actual composition of the ingot was 0.84 mass% cobalt and 0.23 mass% beryllium along with balance of copper by chemical analysis. A bar with a diameter of 16 mm was obtained by subsequent hot forging, thermal extrusion, and cold drawing. The heat treatment of specimens with a size of ϕ16 mm×10 mm was carried out by a KSS-1200 gas protection tube furnace. Based on the phase diagram of Cu-Be alloys[30], the solution temperature of specimens was 950 ℃ and the holding time was 1 h. Then, the specimens were aging treated at 480 ℃, held for 4 h and cooled in air. The performance and microstructure of Cu-0.84Co-0.23Be alloy were related with the process parameters of heat treatment (temperature and holding time).

Mechanical properties of Cu-0.84Co-0.23Be alloy were measured in accordance with the uniaxial tensile test. Tensile samples were prepared according to the GB/T 228.1-2010 tensile testing at room temperature and the GB/T 4338-2006 tensile testing at elevated temperature, respectively. The experimental results of tensile testing were repetitive. Fig. 1 shows the tensile specimens for room temperature tests and elevated temperature tests. Tensile testing for each condition, as well as data acquisition and analysis, was performed using a SHIMADZU AG-I 250 kN precision universal testing machine with a constant strain rate of 2 mm/min. In addition, a high-temperature heating device associated with the testing machine was implemented for elevated temperature tests. The fractured surface morphologies

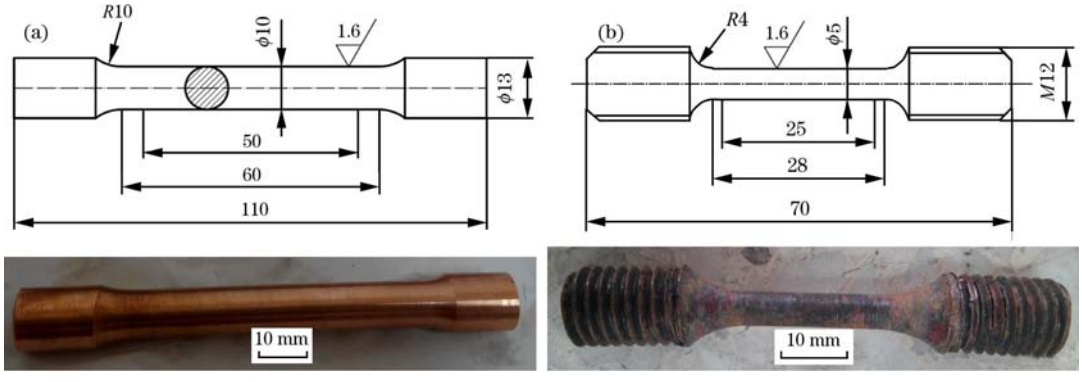

Fig. 1 Drawing of tensile specimens (unit: mm) for room temperature tests (a) and for elevated temperature tests (b)

were observed using a scanning electron microscope (SEM). The specimens were cleaned three times by ethanol liquid in KQ5200 ultrasonic stirrer before SEM observation. The microstructures of supersaturated solid solution and precipitates after solution and aging treatment were observed under a transmission electron microscope (TEM).

2 Results and Discussion

The tensile strength and elongation of Cu-0.84Co-0.23Be alloy under different states are presented in Table 1. Compared with the mechanical properties for drawing state, the tensile strength for solution condition decreases sharply to 271.9 MPa, but the elongation increases significantly from 18% to 42%. The reason is that the Be atoms dissolved into the Cu matrix and formed the supersaturated solid solution after solution heat treatment. Subsequently, the tensile strength of alloy increased significantly and reached a peak value of 580.2 MPa after aging treatment, while the elongation reduced to the minimum value of 4.6%. Although the tensile strength of aged Cu-0.84Co-0.23Be alloy tested at 450 ℃ shows a reduction compared with that of aging state at room temperature, the value is still higher than that of solution state. Furthermore, the elongation has an obvious increase and achieves the value of 11.2% (Table 1).

Table 1 Comparison of experimental results of Cu-0.84Co-0.23Be alloy under different states

State	Test temperature/℃	Tensile strength/MPa	Yield strength/MPa	Elongation/%
Drawing	25	476.6	436.6	18.0
Solid solution	25	271.9	—	42.0
Aging	25	580.2	468.2	4.6
	450	383.6	314.3	11.2

Fig. 2 shows the fracture morphologies at room temperature of Cu-0.84Co-0.23Be alloy under drawing state. Fig. 2(a) shows that the tensile sample has a marked necking phenomenon, and the fracture direction is parallel to the axis of tensile direction. In addition, the fracture surface consists of three distinct regions, i.e. fibrous region, radial region, and shear lip region, which represent the crack initiation, crack extension, and shear fracture zones, respectively. Firstly, fracture occurs in the fiber region and then expands rapidly to the radiation region and break down finally with the formation of shear lips. The radiation direction is the direction of crack source. Figs. 2(b)—2(d) show that the crack zone of

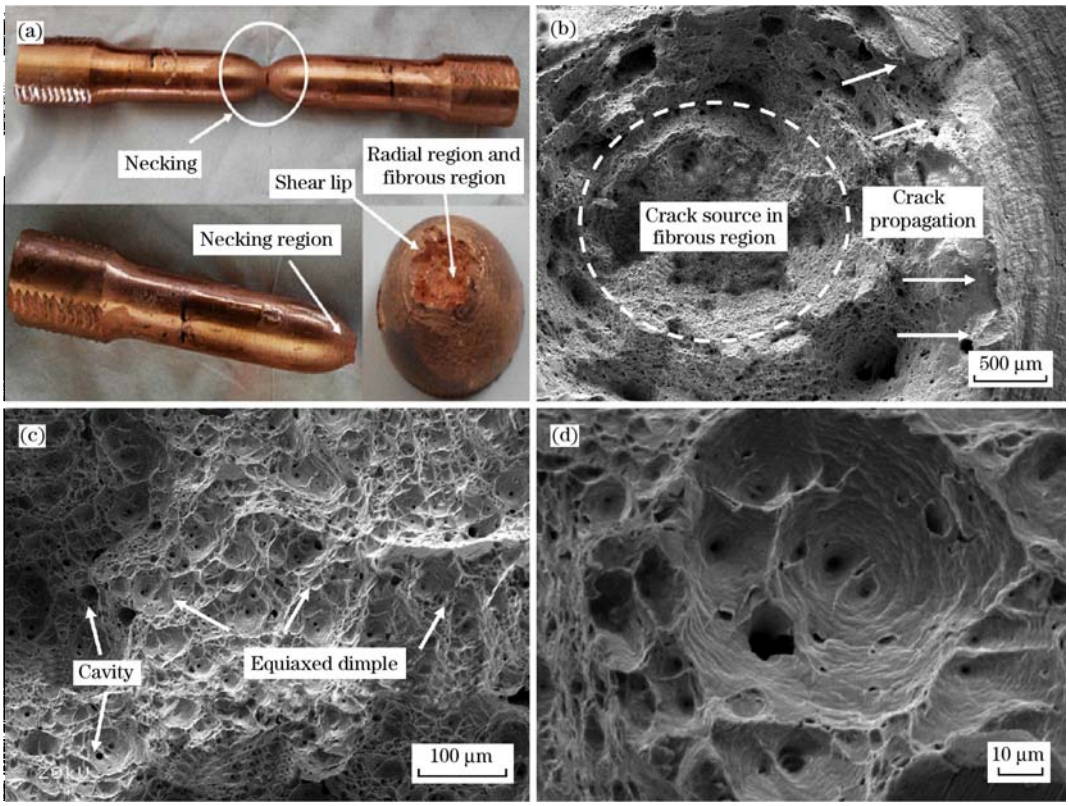

(a) Macroscopic fracture morphology; (b), (c), (d) Microscopic fracture morphologies under different magnifications.

Fig. 2 Fracture morphologies at room temperature of Cu-0.84Co-0.23Be alloy under drawing state

Cu-0.84Co-0.23Be alloy consists of equiaxed dimples and micro-cavity.

The fracture morphologies at room temperature of Cu-0.84Co-0.23Be alloy under solution state are shown in Fig. 3. Fig. 3(a) shows that the as-quenched sample breaks along the angle of 45° to the tensile direction under the action of shear stress. Moreover, the obvious plastic deformation appears near the fracture and the surface of sample has a large number of scaly cracks. As shown in Figs. 3(b)—3(d), in comparison with the equiaxed dimples under drawing condition, the relatively shallow dimples namely parabolic dimple or shear dimple with the parabolic shape distribute on the shear lips zone.

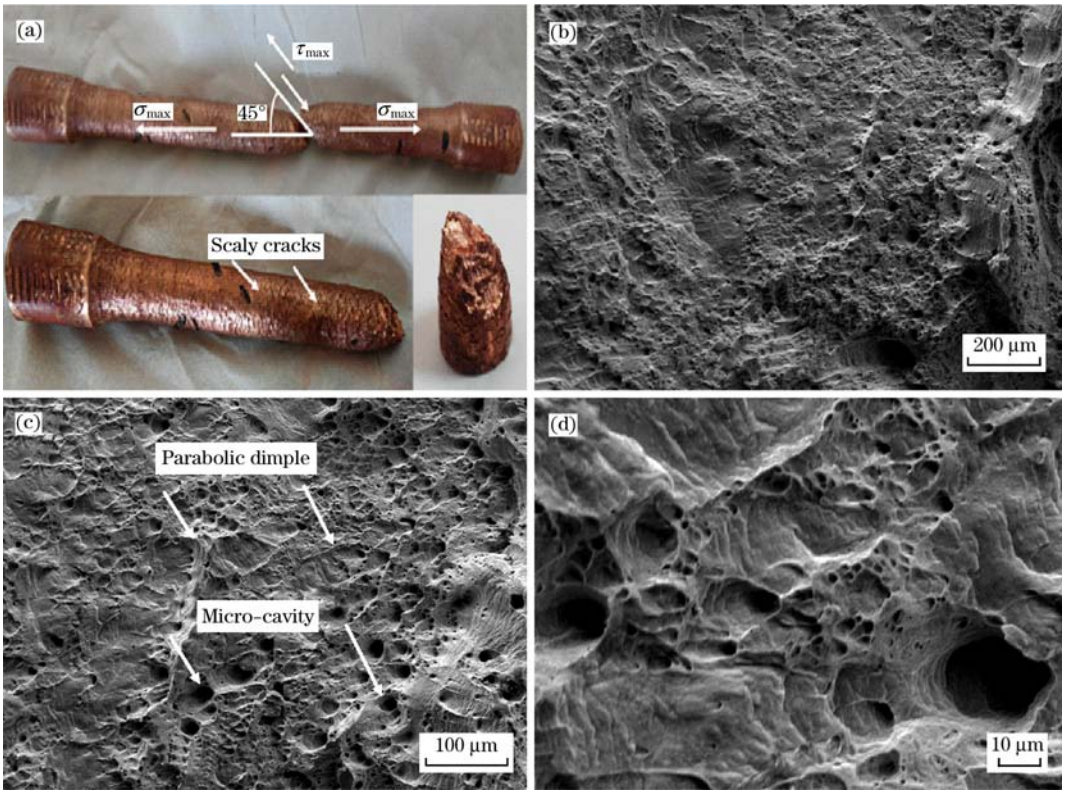

(a) Macroscopic fracture morphology; (b), (c), (d) Microscopic fracture morphologies under different magnifications.

Fig. 3 Fracture morphologies at room temperature of as-quenched Cu-0.84Co-0.23Be alloy at 950 ℃ for 1 h

Fig. 4 shows the fracture images at room temperature of Cu-0.84Co-0.23Be alloy aged at 480 ℃ for 4 h. Fig. 4(a) shows that the failure mode is brittle intergranular fracture. The macroscopic fracture surface is characterized by bright surfaces, and every bright surface is the interface of grains. The fracture cross section is candy-shaped morphology with the coarse grains. According to Figs. 4(b)—4(d), each polyhedron of grain morphology is similar to the gathered candy, and the triple nodes in grain boundary surface are also observed clearly. In addition, partial shallow shear dimples are found on some crystalline grains.

The fracture morphologies of aged Cu-0.84Co-0.23Be alloy after high temperature tensile test at 450 ℃ are shown in Fig. 5. Fig. 5(a) shows that the macroscopic failure mode is also the brittle intergranular fracture. However, owing to the oxidation reaction under high temperature, the interfaces of grains are not as bright as those of samples at room temperature. As shown in Figs. 5(b)—5(d), except for the candy-shaped morphology, more shear dimples and tearing ridges distribute on local crystalline grains (Fig. 5(c)). In addition, a lot of small and deep equiaxed dimples and micro-cavity are also observed, which indicates that the ductility is better in these zones (Fig. 5(d)).

The microstructures of supersaturated solid solution and precipitates after solution and aging treatment are shown in Fig. 6, respectively. Due to the sufficient dissolution of solute atoms in the Cu matrix and rapid cooling rate, the α supersaturated solid solution formed after solution treatment at 950 ℃ for 1 h (Fig. 6(a)). Under as-quenched condition of Cu-0.84Co-0.23Be alloy, the integrity of matrix lattice was destroyed because of the formation of a large

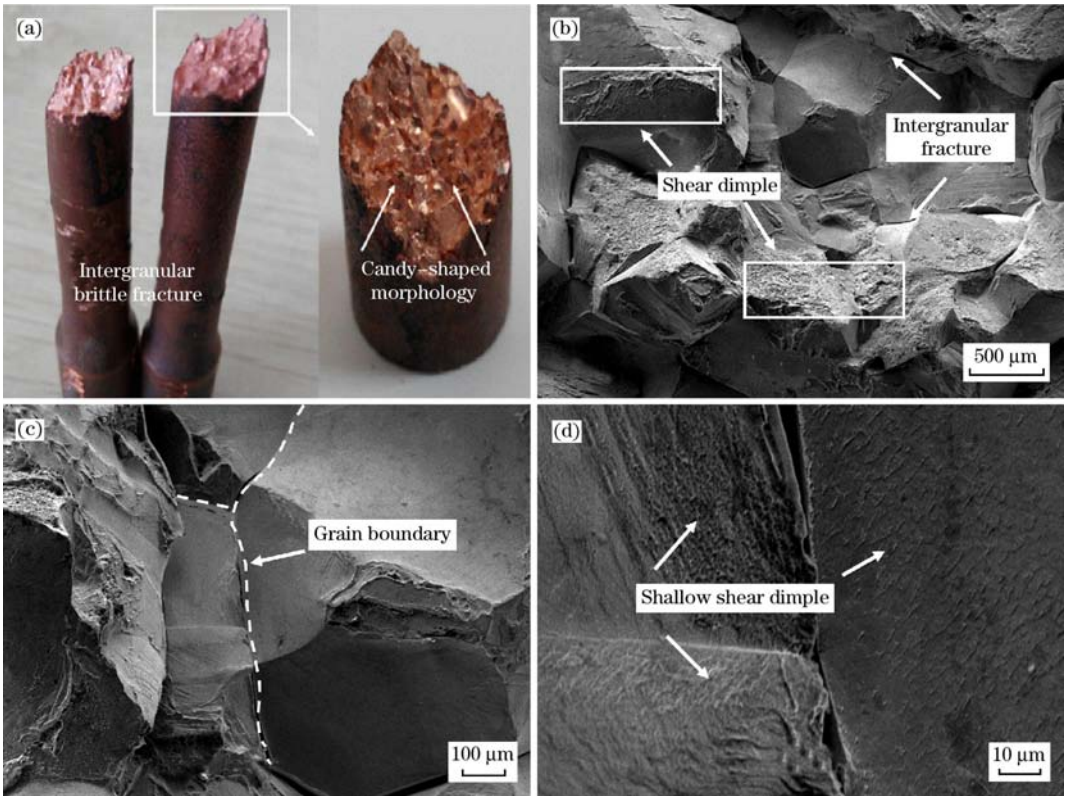

(a) Macroscopic fracture morphology; (b), (c), (d) Microscopic fracture morphologies under different magnifications.

Fig. 4 Fracture morphologies at room temperature of Cu-0.84Co-0.23Be alloy aged at 480 ℃ for 4 h

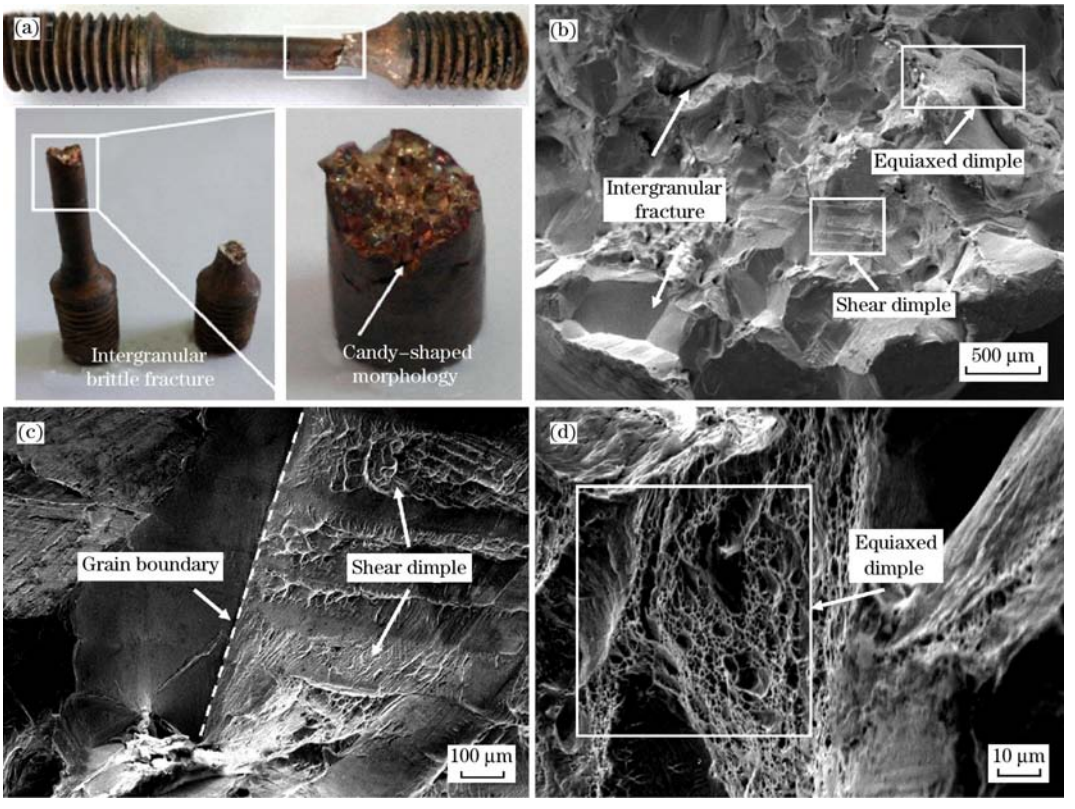

(a) Macroscopic fracture morphology; (b), (c), (d) Microscopic fracture morphologies under different magnifications.

Fig. 5 Fracture morphologies at 450 ℃ of Cu-0.84Co-0.23Be alloy aged at 480 ℃ for 4 h

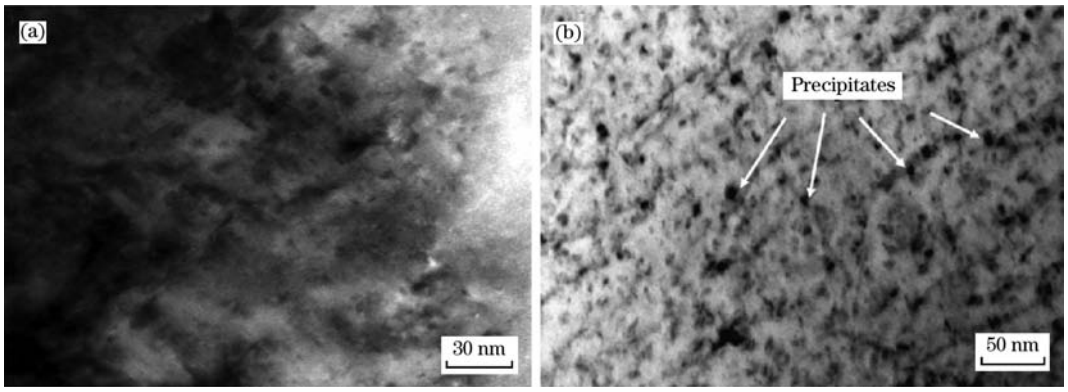

(a) Solution treatment at 950 ℃ for 1 h; (b) Aged at 480 ℃ for 4 h.

Fig. 6 TEM images of Cu-0.84Co-0.23Be alloy after solution and aging treatment

amount of vacancies. The electron wave scattering led to the decrease of conductivity of Cu-0.84Co-0.23Be alloy[31,32]. In addition, the specimens exhibited no detectable precipitation and the low dislocation density showed that no straining during quenching occurred. Therefore, the as-quenched alloy was still relatively soft and had an excellent elongation as well as the relatively lower tensile strength (Table 1). However, a series of phases precipitated from the α supersaturated solid solution and distribute on the copper matrix by the subsequent aging treatment[33,34]. It can be seen from Fig. 6(b) that a large amount of precipitates dispersively distribute on the copper matrix. For Cu-0.84Co-0.23Be alloy, the precipitates effectively hindered the motion of dislocations due to the strong lattice distortion field, and thus led to the improvement of mechanical properties[35,36]. Therefore, the tensile strength of Cu-0.84Co-0.23Be alloy improved significantly after aging at 480 ℃ for 4 h (Table 1).

The fracture morphologies reveal that the failure mode is mainly the ductile fracture. The fracture cross section is perpendicular to or parallel to the tensile stress direction. The micro-fracture morphologies of drawing and solution samples are mainly the equiaxed dimples and the shear dimples, respectively. The difference can be interpreted that the shape of dimples is dominated by the state of sustained stress, and the size as well as the depth related to the ductility of the material. For instance, the equiaxed dimples form under the normal stress. The micro-holes grow around uniformly and the approximate roundness equiaxed dimples occur after fracture under the effect of normal stress (Fig. 2(b)). However, under the shear stress, the shear or parabolic dimples usually occur in the shear lips zones of tensile fracture (Fig. 3(b)). The process of dimples fracture is the formation, growing up, and interconnection of micro-holes. It belongs to a kind of high energy absorption process of ductile fracture. The micro-holes (cavity) form on the area with serious plastic deformation. The inclusions in this area are the nucleation location of micro-cavities. The micro-cavities grow up and gather together, and then lead to the appearance of cracks. The cracks extend rapidly and finally break down in the shear lip area. The main fracture mechanisms of aged Cu-0.84Co-0.23Be alloy at room temperature and high temperature are brittle fracture. The brittle fracture surface is usually perpendicular to the tensile stress direction. The brittle intergranular fracture largely depends on the grain boundary surface states. The precipitation along grain boundary of brittle phase due to metallurgy or heat treatment factors can lead to the crystal brittle fracture. For the Cu-Co-Be alloy aged at 480 ℃ for 4 h (Fig. 6), a series of precipitates form on the grain boundary, and finally result in the intergranular brittle fracture. However, according to the fracture morphologies of specimens for room temperature and elevated temperature tests, the former have a little quantity of shear dimples and the latter have more shear dimples and deep equiaxed dimples (Figs. 4 and 5). The results indicate that the failure mechanism is the multi-mixed mechanism that brittle intergranular fracture plays a dominant role and ductile fracture is secondary. Moreover, the specimens for high temperature test are accompanied by the oxidation reaction.

3 Conclusions

(1) The plastic deformation and heat treatment have significant effects on the tensile proper-

ties of Cu-0.84Co-0.23Be alloy. The experimental results of tensile test are repetitive. For the as-drawing specimens, the tensile strength and elongation are up to 476.6 MPa and 18%, respectively. After solution treatment at 950 ℃ for 1 h, the tensile strength decreases to 271.9 MPa, while the elongation increases to 42%. Furthermore, the tensile strength increases significantly to 580.2 MPa after aging at 480 ℃ for 4 h, while the elongation is only 4.6%.

(2) It is confirmed that the mechanical properties and fracture behavior are dominated by the microstructure characteristics. The failure mode after severe plastic deformation is the typical equiaxed ductile fracture with a marked necking. The fractured surface consists of deep dimples and microvoids. Due to the formation of supersaturated solid solution, the fracture morphologies for solution state are parabolic dimples. During the aging process, a large number of precipitates form and distribute on the Cu matrix. The aged specimens exhibit obvious brittle intergranular fractures.

(3) The tensile strength and elongation of aged Cu-0.84Co-0.23Be alloy for elevated temperature test are 383.6 MPa and 11.2%, respectively. The fractured morphologies are mainly candy-shaped grains with partial parabolic dimples and equiaxed dimples. The fracture mode is multi-mixed mechanism that brittle intergranular fracture plays a dominant role and ductile fracture is secondary.

References:

[1] P. Zhen, Dev. Appl. Mater. 29 (2014) 99-104.
[2] Y. Karaki, Y. Koike, M. Kubota, H. Lshimoto, Cryogenics 37 (1997) 171-172.
[3] A. Woodcraft, R. V. Sudiwala, R. S. Bhatia, Cryogenics 41 (2001) 603-606.
[4] G. L. Xie, Q. S. Wang, X. J. Mi, B. Q. Xiong, J. P. Li, Mater. Sci. Eng. A 558 (2012) 326-330.
[5] R. Monzen, Y. Takagawa, C. Watanabe, D. Terada, N. Tsuji, Procedia Eng. 10 (2011) 2417-2422.
[6] E. A. Smith, Finan. Analyst. J. 16 (1960) 51-54.
[7] P. Behjati, H. Vahid Dastjerdi, R. Mahdavi, J. Alloys Compd. 505 (2010) 739-742.
[8] P. Gallo, F. Berto, P. Lazzarin, P. Luisetto, Procedia Mater. Sci. 3 (2014) 27-32.
[9] L. Yagmur, Mater. Sci. Eng. A 523 (2009) 65-69.
[10] L. Lang, Environ. Health Persp. 102 (1994) 526-531.
[11] W. S. Du, R. Cao, Y. J. Yan, Z. L. Tian, Y. Peng, J. H. Chen, Mater. Sci. Eng. A 486 (2008) 611-625.
[12] L. E. Murr, E. A. Trillo, A. A. Bujanda, N. E. Martinez, Acta Mater. 50 (2002) 121-131.
[13] A. Shokuhfar, O. Nejadseyfi, Mater. Sci. Eng. A 594 (2014) 140-148.
[14] J. Cao, F. G. Li, P. Li, X. K. Ma, J. H. Li, Mater. Sci. Eng. A 637 (2015) 201-214.
[15] O. Sabokpa, A. Zarei-Hanzaki, H. R. Abedi, Mater. Sci. Eng. A 550 (2012) 31-38.
[16] N. Subrahmanya Prasad, N. Naveen Kumar, R. Narasimhan, S. Suwas, Acta Mater. 94 (2015) 281-293.
[17] M. Sharififar, S. A. A. Akbari Mousavi, Mater. Sci. Eng. A 594 (2014) 118-124.
[18] K. V. Sudhakar, J. C. Cisneros, H. Cervantes, C. G. Pineda, J. Mater. Eng. Perform. 15 (2006) 117-121.
[19] Y. Rosenthal, J. Mater. Sci. 27 (1992) 2193-2198.
[20] K. P. Jen, L. Q. Xu, S. Hylinski, N. Gildersleeve, J. Mater. Eng. Perform. 17 (2008) 714-724.
[21] J. C. F. Millett, Metall. Mater. Trans. A 46 (2014) 4506-4517.
[22] Z. H. Feng, X. J. Jiang, Y. K. Zhou, C. Q. Xia, S. X. Liang, R. Jing, X. Y. Zhang, M. Z. Ma, R. P. Liu, Mater. Des. 65 (2015) 890-895.
[23] O. Satoshi, M. Naokuni, S. Kazumasa, W. Chihiro, M. Ryoichi. J. Soc. Mater. Sci. 56 (2007) 531-537.
[24] J. C. Pang, Q. Q. Duan, S. D. Wu, S. X. Li, Z. F. Zhang, Scripta Mater. 63 (2010) 1085-1088.
[25] Y. C. Tang, Y. L. Kang, L. J. Yue, X. L. Jiao, Mater. Des. 85 (2015) 332-341.
[26] R. Monzen, T. Hosoda, Y. Takagawa, C. Watanabe, J. Mater. Sci. 46 (2011) 4284-4289.
[27] J. P. Li, B. Q. Xiong, G. L. Xie, Q. S. Wang, B. H. Song, Rare Met. 32 (2013) 332-337.
[28] J. C. Rebelo, A. M. Dias, R. Mesquita, P. Vassalo, M. Santos, J. Mater. Process. Technol. 103 (2000) 389-397.
[29] L. Yang, F. Y. Zhang, M. F. Yan, M. L. Zhang, Appl. Surf. Sci. 292 (2014) 225-230.
[30] D. J. Chakrabarti, D. E. Laughlin, L. E. Tanner, Bull. Alloy Phase Dia. 8 (1987) 269-288.
[31] G. Sha, A. Cerezon, Acta Mater. 52 (2004) 4503-4516.
[32] S. D. Liu, C. B. Li, S. Q. Han, Y. L. Deng, X. M. Zhang, J. Alloys Comp. 625 (2015) 34-43.
[33] A. Bachmaier, G. B. Rathmayr, M. Bartosik, D. Apel, Z. Zhang, R. Pippan, Acta Mater. 69 (2014) 301-313.
[34] M. Dellah, M. Bournane, Kh. A. Ragab, Y. Sadaoui, A. F. Sirenko, Mater. Des. 50 (2013) 606-612.
[35] A. K. Shukla, S. V. S. Narayana Murty, S. C. Sharma, K. Mondal, J. Alloys Compd. 590 (2014) 514-525.
[36] G. Kurtuldu, P. Jessner, M. Rappaz, J. Alloys Compd. 621 (2015) 283-286.